A Novel Fault Detection and Fault Location Method for Multi-Terminal HVDC Transmission Lines Based on Gap Frequency Spectrum Analysis

Qingqing Yang, Simon Le Blond, and Jianwei Li

Abstract: This paper proposes a novel protection scheme for multi-terminal High Voltage Direct Current (MTDC) systems based on high-frequency components detected from the fault current signal. This method can accurately detect the fault on each line and classify the fault types. Using the post-fault current time series, both single-ended measurements (detection and classification) and double-end measurements (location), the frequency spectrum is generated to measure the gaps between the contiguous peak frequencies giving a robust and comprehensive scheme. Unlike the previous travelling wave based methods, which must identify the travelling wavefront and require a high sampling rate, the new gap-based approach is able to give accurate fault detection and fault location using any appropriate range of post-fault signals. Furthermore, the proposed method is fault resistance independent and thus even a very high fault impedance has no effect on the fault location detection. A three-terminal VSC-HVDC system is modelled in PSCAD/EMTDC software, which is used for obtaining the fault current data for the transmission line terminal. The algorithm is verified by studying a range of cases, by varying the fault resistance fault locations and also including external faults. The results show that the proposed method gives an accurate and reliable fault detection, classification and location on the test MTDC system. In addition, the proposed algorithm can potentially be used in other HVDC or MTDC systems.

Keywords: Fault current signal, fault detection, fault location, transmission line, VSC-HVDC system.

1 Introduction

Sources of renewable energy are often available in remote locations, and so must be transported over long distances to supply load centres [1, 2]. The development of power system technology and the increasing penetration of renewable energy has led to interconnected national grids, resulting in increasingly economic and sustainable electrification worldwide [3]. Consensus on climate change mitigation in Europe has led to a new target of 27% renewable sources by 2030 [4]. One of the solutions to such ambitious targets may be HVDC super-grids, used to connect large numbers of offshore wind farms or transporting photovoltaic from desert regions [5].

The recent technological advancements in power electronics and circuit breakers make MTDC transmission a promising technology [6, 7]. In particular the advantages of VSC-based HVDC technology increase the feasibility of multi-terminal systems [8]. However, many challenges remain in the evolution from point-to-point HVDC to multi-terminal HVDC, especially in protection design. The objective of a protection scheme is to keep the wider system stable by de-energising and isolating the minimum possible plant and leaving as much of the healthy network still in operation [9]. In typical HVDC point-to-point links, the most

common approach is using AC circuit breakers, tripping the entire HVDC system from the AC grid. Hence, the circuit breakers reside on the AC side, and in the event of a fault, the entire link is de-energised [10]. In the multi-terminal case, however, it is more desirable to isolate only the faulted link rather than trip the entire DC grid. Therefore, DC circuit breakers have been developed to isolate the faulted line, but their operation must be controlled by DC protection relays. An accurate fault location must be used to help restore the system to a normal operating condition [3] and fix permanent faults. Due to fundamental differences in system operation, DC protection relaying requires special consideration over conventional AC methods. In particular, conventional impedance locus based distance protection is not appropriate for DC systems because the line impedance is one dimensional.

Currently, travelling wave based methods as introduced in [3, 11, 12], are the most common HVDC and MTDC transmission line protection. Such approaches are very fast and reasonably accurate and work through detecting initial wave front of the voltage or current fault surge. The discrete wavelet transform (DWT) is usually chosen over pure frequency or time-domain based methods, because of its fast computational time and straightforward implementation [13]. For example in [14] two out of three of the fault criteria are determined with the DWT and used together with a time domain method. However, the travelling-wave principle must make use of a high sampling rate and relies completely on accurate wave front detection. Boundary protection has been proposed in [15]. Based on boundary characteristics, another transient harmonic current protection method is introduced in [16]. Differential protection is also applied to HVDC transmission lines [17] but relies on two terminal measurements and a communication link between them. Other specific methods have been developed such as fault location using the similarity of voltage signals [18]. Extracting the natural frequencies is introduced in [19], which uses the natural frequency generated by travelling wave, although a higher resolution spectra estimation tool is required. Sheath voltage can be used as criteria for fault detection and classification [20]. A method using frequency, time and energy to capture the fault features is presented in [21]. ANN based methods can be also applied in HVDC and multi-terminal HVDC systems [22]. However, all such aforementioned methods have at least one of the following drawbacks, such as, relying on two-terminal measurements, slow operation, poor robustness (for example, dependability with high impedance faults) or lack of proven generality.

The speed of operation has a strict requirement for a DC protection system, with fault clearing times within several milliseconds. The fault must therefore be cleared quickly to avoid damage to the sensitive power-electronic equipment and to keep the fault current below the maximum interruptible current of dc breakers [23]. As proposed in [24], the frequency spectrum of voltage and current is a useful source of information for protection purposes. As introduced in [25], the high-frequency component is a good criterion for fault detection and fault location. This paper presents a new frequency domain method using features in the transient fault current spectra. Fault detection and classification is achieved quickly and robustly using a one terminal measurement and fault location is then achieved reliably using two terminal measurements.

2 Theory of Proposed Method

2.1 High-frequency component

When a fault causes a step change in the circuit, a wave travels out from the fault point close to the speed of light in a vacuum and is reflected at the discontinuities in the line, causing high-frequency components. Travelling waves measured at the relaying point are seen as high-frequency oscillations.

Such generated travelling waves consist of natural frequencies, which can be regarded as

Commented [SLB1]: What are these special considerations?

Commented [SLB2]: You should really add the drawbacks of all these existing methods to justify why your scheme is better.

Commented [SLB3]: See comment above.

a series of frequency components with equal distance. Unlike existing research [19, 26], which relies on the dominant frequency component, this paper presents an approach using the characteristic of equal distance between the high-frequency components in the post fault spectra [27].

The frequency content during a fault on the transmission line is observed to change depending on the fault characteristics, and thus can be used to obtain information about the fault. Due to the large DC component, frequencies higher than 700 Hz are used in the new scheme. This is extracted from the fault current signals using the Fast Fourier Transform.

Unlike travelling wave methods which rely on the detection of the wave-front, the new fault detection and location can use any parts of the post fault signal which contain features due to the propagation of the travelling waves. Additionally, the high-frequency contents have features at locations on spectra that vary with fault location, but are importantly independent of fault resistance.

Commented [SLB4]: Reference your earlier paper here or thesis?

2.2 Travelling wave principle

A fault on the transmission line will result in travelling waves on both current and voltage signals, and will travel in both directions originating from the fault position. The propagation of the wave and subsequent reflections can be clearly analysed in space and time using a Bewley Lattice diagram. At any point on the transmission line, the current and voltage at point x can be described with the partial differential equations (1).

$$\begin{cases} \frac{\partial_e}{\partial_x} = -L\frac{\partial_i}{\partial_x} \\ \frac{\partial_i}{\partial_x} = -C\frac{\partial_e}{\partial_x} \end{cases} \quad (1)$$

Where: L is the line inductance, C is the capacitance, e and i represent the voltage and current at the location x.

The current signal, which has both a time and distance dependency, is described by (2).

$$i(x,t) = \frac{1}{Z}[e_i(x-vt) + e_r(x+vt)] \quad (2)$$

Where: $Z = \frac{1}{\sqrt{L/C}}$ that Z is the characteristic (surge) impedance of the transmission line, $v = \frac{1}{\sqrt{LC}}$ is the velocity, e_i and e_r are two arbitrary functions of $(x-vt)$ and $(x+vt)$, which refer to the incident and reflected traveling wave.

Assuming the fault occurs at t_0, the initial travelling wave is generated by the fault, so the superimposed voltage is:

$$e_k = -\frac{1}{Z}e_f sin(\omega t) \quad (3)$$

Where: e_f is the amplitude of the superimposed voltage.

The propagation of the fault travelling wave is described by 4:

$$\begin{cases} i_a(t) = \frac{1}{Z_C}\begin{bmatrix} -e_k(t-\tau_a) + K_a e_k(t-\tau_a) + \\ {K_a}^2 e_k(t-3\tau_a) - {K_a}^2 e_k(t-3\tau_a) \ldots \end{bmatrix} \\ i_b(t) = \frac{1}{Z_C}\begin{bmatrix} -e_k(t-\tau_b) + K_b e_k(t-\tau_b) + \\ {K_b}^2 e_k(t-3\tau_b) - {K_b}^2 e_k(t-3\tau_b) \ldots \end{bmatrix} \end{cases} \quad (4)$$

Where: K_a and K_b is reflection co-efficient, $\tau_a = \frac{t_{a2}-t_{a1}}{2}\tau_b = \frac{t_{b2}-t_{b1}}{2}t_a$ and t_b is the wave travel time from the fault to the end of the line.

Commented [SLB5]: Check all equations carefully.

2.3 Fast Fourier Transform

Fourier analysis has a high level of technical maturity, with the Fourier transform being one of the most common techniques used for a variety of measurements in control and protection applications [28]. Specifically, the Fast Fourier Transform (FFT) is a computationally efficient algorithm to convert time-domain signals to their representation in

the frequency-domain. An adequate representation in the frequency domain may be presented by the FFT with a very short window length (<1 s) [29]. In addition, a faster computational time is expediential to meet the time requirement of DC circuit breakers.

Using the Fast Fourier Transform is also an effective way to analyse the features generated by the fault. The basic form of the FFT is given by (5):

$$F(\omega) = \frac{1}{N}\sum_{t=0}^{N-1} f(t)\, exp\left(\frac{-j2\pi\omega t}{N}\right) \quad (5)$$

Where: F(ω) is the spectral component or harmonic, f(t) is the signal sample sequence, N is the number of sample values in each period of the signal.

Using Euler's equation, (5) can be split into real part and imaginary parts.

$$exp\left(\frac{-j2\pi\omega tj}{N}\right) = cos\left(\frac{2\pi\omega t}{N}\right) - jsin\left(\frac{2\pi\omega t}{N}\right) \quad (6)$$

The equation can be rewritten as:

$$F(\omega) = \frac{1}{N}\sum_{t=0}^{N-1} f(t)\left(cos\left(\frac{2\pi\omega t}{N}\right) - jsin\left(\frac{2\pi\omega t}{N}\right)\right) \quad (7)$$

The frequency f versus the peak frequency magnitude is selected for use in fault location. In frequency domain, it can be expressed:

After extensive analysis it was found that in the frequency domain, the frequency value of the peak magnitudes were closely related to the travelling wave arrival time, which in turn is related to the location of the fault. It can be observed that the frequency peaks, which are proportional to travel time, can be described as follows:

$$f_n = f_o + \frac{n}{\tau} \quad (8)$$

Hence, the gap of the peak frequency can be written as:

$$\Delta f = f_2 - f_1 = \frac{1}{\tau} \quad (9)$$

The relationship of the distance and frequency can be expressed in (10), so the distance can be calculated by:

$$x = \tau v = \frac{vn}{f_n - f_o} \quad (10)$$

2.4 Standard Deviation

Through measuring variability or statistical dispersion, the features of a frequency spectrum can be expressed by a number and easily be used as a criterion for fault detection.

Thus if $X(i)$ is a discrete spectrum with N unique points, high frequency measuring can be expressed in (11):

$$HFC = \sum_{i=1}^{N} i|X(i)| \quad (11)$$

The standard deviation (SD), is a measure that is used to quantify the amount of variation or dispersion of a set of data values. Hence, the standard deviation of the frequency spectrum can be presented as S_f given by (12)

$$S_f = \sqrt{\frac{1}{N-1}\sum_{i=1}^{N}(X_i - \mu)^2} \quad (12)$$

Where: $\mu = \frac{1}{N}\sum_{i=1}^{N} x_i$ is the standard value of samples, N is the total number of data, X_i is the value of the ith data point.

An advanced deviation method based on standard deviation is used for fault location in this paper, which can be used to separate the external AC fault, the terminal fault and the internal DC transmission line fault. These methods are based on estimating the sample standard deviation about the mean of a specified range of frequency spectrum over a moving current signal window. For external faults, there is no influence in the high-frequency component generated by a travelling wave, so that the change in frequency spectrum is similar to the cases of no fault. This is thus the criterion used to detect whether the disturbance is external or within the protected zone in the new scheme presented in this paper.

Commented [SLB6]: Do you mean 1 ms here?

Commented [SLB7]: Missing equation?

3 Protection Scheme

3.1 Fault Detection

The new protection scheme is based on the transient signal by measuring the high-frequency transient current on transmission line during a fault. Transient-based protection techniques are well known and have been successfully used for power line protection and fault location that is robust to fault path impedance, power swing and CT saturation [30].

It is crucial to measure the signal from the system and extract the features from the frequency domain signal in the protection scheme. Hence, signal processing is required. Through signal processing, the signal has a certain ability to sustain noise, even though the direct use of the measured signal is straightforward and fast [14].

The fault current is generally affected by fault types, fault location on the transmission line, ground impedance, short-circuit capacity and other factors like converter stations. In addition, some faults are caused by the disconnection of a DC transmission line. During a fault, these disturbances will be expressed by the transient signal detected on the terminals which contain many characteristic frequencies. The high-frequency component is considered to be the most significant factor in this paper is because the frequency components are more likely to be influenced by fault location rather than other factors like fault resistance.

It is assumed that DC circuit breakers are located at both ends of each line to trip the faulted line following a fault. Current DC circuit breakers must be triggered within a few milliseconds (about 5 ms) [31]. The main protection should be as fast as possible to meet the protection requirement which is assumed to be 5 ms in this paper, with identical protection functions fed from separate instrument transformers. Unlike the two-ended methods which require the communication system and synchronized timer, here one-end fault detection is presented which gives overall faster response. The flowchart of fault detection is shown in Fig. 1.

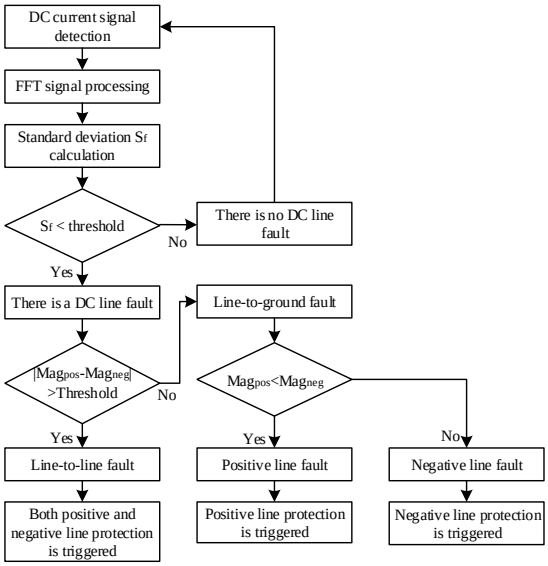

Fig. 1 Flowchart of fault detection

The criteria for fault detection and fault location are based on the frequency spectrum detected by only the fault current signal. In the presented fault detection method, a 1 ms window, which causes the greatest delay in the fault detection process, is applied to the faulted current signal. Through FFT analysis, the fault current signal is transformed from

Commented [SLB8]: Why do you need separate primary sensors – surely you just feed the same signal and do the relaying logic in parallel?

Commented [SLB9]: I would suggest change to "The main protection should be as fast as possible to meet the protection requirement which is assumed to be 5 milliseconds in this paper. Thus signals from instrument transformers are sent to relays with parallelised protection logic. "

time-domain to frequency-domain using equation (5). A selected frequency band is calculated by equation (12) to obtain the standard deviation. The criterion in zonal fault detection is the proportion of standard deviation of the selected range of frequency spectrum in the mean value.

$$S_f/M_f < S_{setting} \tag{13}$$

Where: S_f is the standard deviation of the selected range of dara, M_f is the mean value of the selected data, $S_{setting}$ is the threshold of the fault detection algorithm.

Fault classification then follows to diagnose if the fault involves one pole and ground or both the positive pole and the negative pole. The criterion is based on the differences between the spectra. In the case of a line-to-line fault there will only be a slight difference in the travelling wave spectra on both poles. However, with a line to ground fault, the healthy pole will have very little high frequency content since there are no travelling waves. Thus if the differences between the spectra are found to be below a pre-determined threshold, a line-to-line fault is diagnosed, and in the opposite case, a line-to-ground fault is diagnosed.

3.2 **Fault Location**

Once the fault is detected and classified, the fault location is activated. In the fault location algorithm, a 10 ms window for signal detection is used to obtain a sufficiently long fault current signal. A frequency spectrum is generated using the fast fourier transform, ready for peak analysis.

Peak Analysis is essential step in fault location algorithm in this paper. In the data processing stage, the peaks in the frequency spectrum must be detected along with their frequency value. Peak value in this paper is defined as the frequency at which the frequency spectrum reaches its maximum magnitude within a specified frequency range. Peaks in the frequency spectrum signals seem to appear at regular intervals. However, the presence of random noise in the real experimental signal, which is mainly caused by adjacent busbar and transposed transmission lines, and non-ideal instrument transducers [32], will result in smaller false peaks. These pseudo peaks are generally very close to the real peaks. Thus, to avoid mal-operation, the first step for signal processing is to smooth the target signal. A smoothing filter is thus applied to the frequency spectrum with a very fast computational time. The smoothing process may give some distortion for target data with only one or two peaks, however, it is effective for data with several peaks.

In peak analysis, specific parameters particular to the MTDC system must be quantified in accordance with the characteristics of the particular fault current frequency spectra.

The mean value of the gap between two adjacent peak magnitudes is:

$$G = \frac{f_m - f_n}{m-n} \tag{14}$$

Where: G is the gap between two frequency bands.

The simplified fault location equation can be written using the one-end data and two-end data in the equation (15):

$$D = \mu/G_1 \tag{15}$$

Where: $D = \frac{G_2}{G_1+G_2}$ is the fault location, μ is a coefficient determined empirically by careful study of the spectra for the specific system, G_1 is the average value of gap between frequency bands in terminal 1, G_2 is the average value of gap between frequency bands in terminal 2. Using the proportionality for fault location is benefcial because it is independent of the length of transmission line and the system parameters.

Inter-terminal communication necessary for two ended scheme is handled by communication boards in protection cubicles with communication links using high-speed links obtained with optical fibre connections.

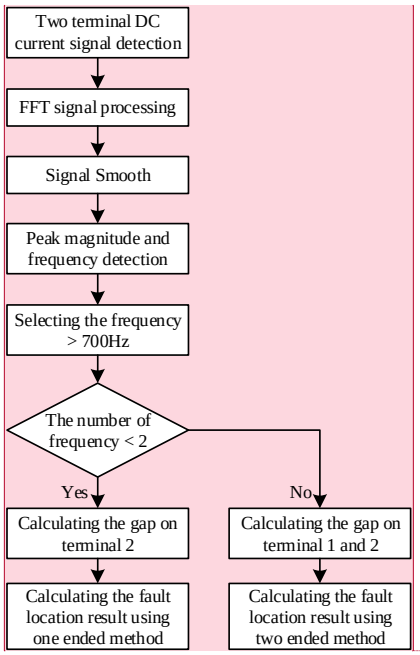

Fig. 2. Flowchart of fault location

The flowchart of fault location is shown in Fig. 2. The current transient signal is detected with a 10 ms window on both ends of the transmission line. Using the FFT, the frequency spectrum is generated for peak detection. To mitigate the influence of the pseudo-peak frequency, signal smoothing is achieved with a smoothing filter applied to the frequency spectra and not the original time series. Then all frequencies below 700 Hz are discarded - this process effectively acting like a high-pass filter. After the frequencies with peak magnitude are detected, the system will determine if there are two spectra for two-ended calculation. If there has been time to collect and process a spectrum from the remote terminal, the more accurate two-end data equation will be employed, otherwise, if the communication link fails, or is too slow, the one-end method will be applied. Reverting to a single ended calculation is necessary for a long transmission line when the fault occurs very near the remote terminal.

4 Simulation Test

4.1 Multi-terminal System Modelling

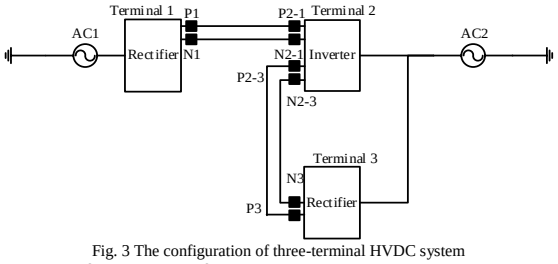

Fig. 3 The configuration of three-terminal HVDC system

Fig. 3 illustrates the configuration of a three-terminal HVDC system which is designed

Commented [SLB10]: Change the “The number of frequency <2” to “The number of spectra <2”

based on CIGRE B4 programme described in [22, 33], and simulated in PSCAD/EMTDC software. Other than using cables in the transmission system, 1000 km long overhead line with a distributed parameter, frequency-dependent model, which is illustrated in Fig. 4, is adopted in this paper. Each converter unit consists of a VSC unit, phase reactor, filter capacitor and an interfacing LTC transformer to connect to the high-voltage AC network.

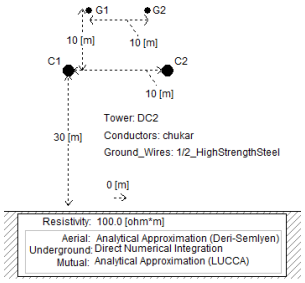

(a) The configuration of overhead transmission line

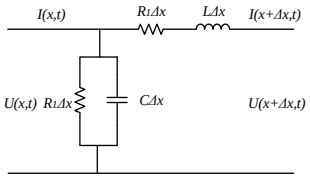

(b) The equivalent circuit for an elemental section of frequency-dependent transmission line

Fig. 4 The overhead transmission line model

The power flow model of a full VSC station is derived first and then used to build the model of the most basic multi-terminal VSC-HVDC system, which is a three-terminal system. The formulation presented here can be extended to a multi-terminal VSC-HVDC system having any number of converter stations and an arbitrary DC topology.

The transmission line or cable can be represented by series impedances and shunt admittances per unit length. The series impedance depends on the frequency because of the inherent frequency dependence of capacitance and inductance and the skin effect of the conductor and earth. Based on these parameters the characteristic parameters of the line surge-impedance and propagation constant-can be derived, which determine the propagation behaviour of travelling waves on the line [34].

On the AC side, phase reactors act as AC filters to reduce the AC current high-frequency harmonic contents caused by the switching operation of the converter station. With the development of two-level converter stations, a low-pass LC-filter on the AC side suppresses high-frequency harmonic components and avoids interaction of fundamental frequency components. DC capacitors are used both for the energy storage VSC topology, and equipped on DC side as filters, and reduce harmonic coupling between two adjacent VSC converter stations that are connected to the same DC bus [35]. DC cables naturally attenuate low-frequencies, but can amplify the high-frequency contents [35].

Although high-frequency components on healthy lines will be caused by faults on nearby lines, particular frequency characteristics are unique only for faults on the measured line, so faults on other external lines will not cause false detection.

4.2 Fault detection and classification result

Based on the modelled system, the sampling frequency is 10 kHz. The fault is applied at 6 s and lasts 0.1 s. To verify the change of frequency spectrum in different fault types, the fault is applied on the negative line in section 1 as an example. Fig. 6 shows the measured

Commented [SLB11]: Is this the simulation frequency or the sampling frequency of the simulated system (simulation bandwidth/stepsize)? From below it looks like the sampling frequency. You should probably therefore say that the system was simluted at a step size of 100 kHz too.

criteria value in different situations.

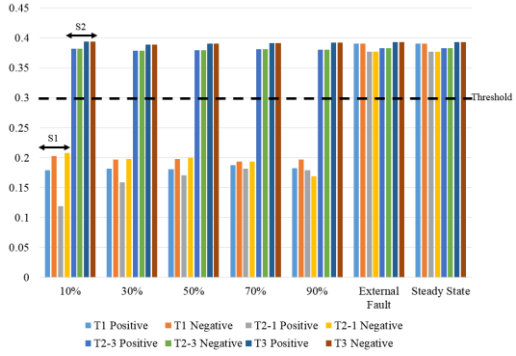

(a) The standard deviation for different fault location

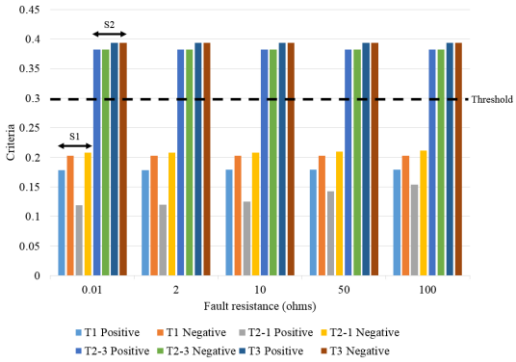

(b) The standard deviation for different ground resistance

Fig. 5 Fault detection for internal fault and external fault with different fault location and different fault resistance

As can be seen in Fig. 5 (a), with the same fault resistance, the result calculated on section 1 is lower than the threshold whereas the result calculated on section 2 is higher than the threshold. In Fig. 5 (b), with different fault resistance, the detection of the fault presents the same result. It can be concluded that the faulted line (S1) can be detected very easily and accurately. Also, an internal fault can be distinguished from an external fault.

Following the flowchart presented in Fig. 1, the fault classification follows from fault detection. By comparing the positive line value with the negative line value, the difference is larger than the set threshold, which suggests a line-to-ground fault occurring on the faulted line. Since the negative line has more high frequency content than the positive line, this signifies a negative line fault. Using this simple comparison gives robust classification of faults.

Commented [SLB12]: Would be good to say exactly what this threshold is for this particular system to give an indication.

4.3 Fault Location

The sampling frequency of 10 kHz was found to be sufficient which is 200 samples per 50 Hz AC cycle. 10 kHz sampling frequency gives the right balance between accuracy and speed, resulting in a detection and location operation time of 1 ms and 10 ms respectively. Through signal processing by FFT analysis, the frequency spectrum is generated in Fig. 6. From (a) to (e) the frequency change related to fault location and the magnitude of fault resistance may be clearly observed. The location of the peaks do not change with fault resistance, only the level of the frequency spectrum, whereas the location of peaks *do* change with the location of the fault.

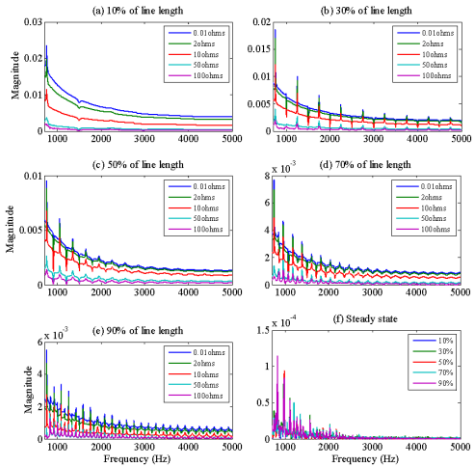

Fig. 6 Frequency spectra for different fault locations from the rectifier, varied from 10% (a) to 90% (e) and frequency spectra in 0.01 W fault resistance (f).

Fault location is based on the detection of the adjacent frequency spectrum. The detection of these high-frequency peaks is shown in Fig. 7. Peak detection, which is integral to the algorithm, is achieved by peak finder in MATLAB with subsidiary conditions applied in the algorithm. As can be seen in the Fig 8, the peaks for all spectra are detected by inspection. The pseudo peaks are filtered not to affect the real peak detection.

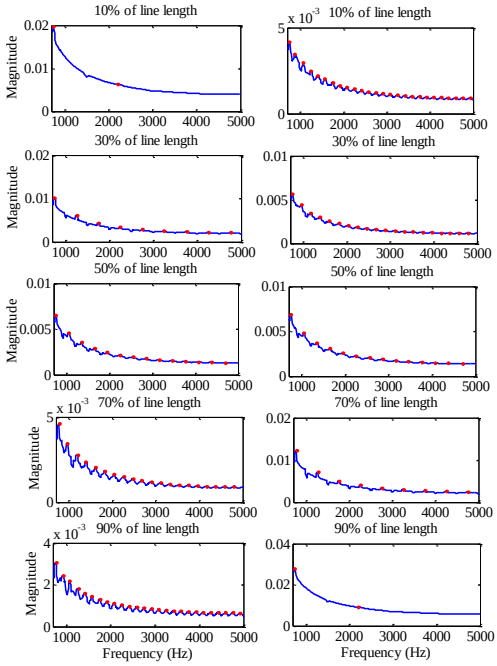

Fig. 7 Peak detection in frequency spectrum

Simulations were done on various types of faults occurring in different locations with different fault resistance. Table 1 lists some example results from different samples, fault

location, fault types and fault resistance.

TABLE I
RESULT OF PEAK DETECTION

Case	Sample	Section	type	Location	Fault resistance	Ip1		In1	
						Number	Average value	Number	Average value
1	1	1	PG	10%	2	2	1480	26	167.6
2	1	1	NG	30%	100	9	501.25	20	213.684
3	1	2	PN	50%	50	14	304.615	14	304.615
4	1	2	PG	70%	10	20	211.579	9	497.5
5	1	2	NG	90%	0.01	26	166	2	1460
6	2	2	PG	70%	100	20	212.63	9	477.5
7	3	1	NG	90%	10	25	167.5	2	1460
8	3	2	PN	30%	2	9	510	19	207.78
9	1	1	PN	1%	0.01	N/A	N/A	28	152.6

According to the proposed method expressed in the flowchart shown in Fig. 2, the fault location result is calculated, which is shown in Table 2 with the two-end method and in Table 3 using the single-end method. The accuracy of the method has been evaluated with (16) to calculate the relative error:

$$e = \left|\frac{D_{act}-D_{det}}{L}\right| \quad (16)$$

Where: D_{act} is actual fault location from the measuring terminal, D_{det} is the detected fault location and L is the total length of the transmission line.

TABLE II
FAULT LOCATION RESULT USING TWO-END METHOD

Case	Actual distance	Measuring distance	Error
1	10%	10.17%	0.17%
2	30%	29.89%	-0.11%
3	50%	50%	0%
4	70%	70.16%	0.16%
5	90%	89.79%	-0.21%
6	70%	69.19%	-0.81%
7	90%	89.71%	-0.29%
8	30%	29.94%	-0.06%
9	1%	1.70%	0.7%

The results show that the proposed method can accurately locate faults with the largest relative error, calculated by (7), being less than 1.05% no matter what fault resistance is, which is in an acceptable range. Comparing two-end method result and one-end method result, the detection of high-frequency component both have a good performance.

Commented [SLB13]: Excellent performance

Commented [SLB14]: Err…Surely the highest value in the table above is 0.81%??? Was this for single ended error?

Commented [SLB15]: You cannot really make this claim unless you give results for the single ended method

5 Discussion

External faults occurring outside the protected lines must be distinguished from internal faults. With the presented fault detection based on standard deviation, external faults can be distinguished from internal faults very reliably.

To design the location algorithm based on the relationship between fault location and frequency components, the test system was simulated with a series fault location (1%, 10%, 30%, 50%, 70%, 90%,). Each fault location has specified features occurring at specific frequencies, and the relationship between fault location and frequency can be expressed by the frequency gap between two contiguous peak magnitudes.

High impedance faults are generally challenging for many protection strategies because of the attenuation of the post-fault characteristics and thus its resemblance to steady state pre-fault conditions. For example, it is difficult to detect high impedance faults reliably with overcurrent characteristics due to very low fault currents.

To test the sensitivity of the new method to fault resistance, the simulation work includes a range of fault resistances from 0.01 Ω to 100 Ω . As can be seen in the frequency spectrum transferred from fault current signal in Fig. 6, the relevant frequency feature can still be obtained under high fault resistances. Even though there known challenges for fault detection and location for faults with high ground resistance, the performance of the new scheme is shown to be very reliable and accurate.

Different sampling frequencies were tested to discern the lowest sampling frequency that the new scheme could operate with. It was shown that sampling frequencies of greater than 5 kHz are required to ensure the accuracy of the scheme. Compared with the travelling wave based fault location method using 192 kHz sampling frequency in [15], the proposed method in this paper uses a relatively low sampling frequency of 10 kHz.The new method was also shown to be robust to noise. White noise with 50 dB SNR was added to the dc current and the frequency spectra generated before and after denoising had the same response to the fault location algorithm.

6 Conclusion

This paper presents a novel protection scheme based on high-frequency component which is generated from fault current signal for the multi-terminal system. A three-terminal VSC-based HVDC model based on CIGRE B4 programme is implemented in PSCAD/EMTDC with different types of faults simulated in the DC transmission system. Fault current signals are detected on all terminals in order to create frequency spectra, giving insights into the characteristic frequency components contained within the signal. The fault detection algorithm can both distinguish the external fault from internal fault, and classify the internal fault for both line-to-ground fault and line-to-line fault within 1 ms. Through the relationship between frequency component and the fault location, a novel location algorithm is proposed based on the gap of two contiguous peak frequencies using either two-end data or one-end data. Very positive test results are shown in the simulation work with accuracy of location to within X.XX%. The most important achievement presented in this protection scheme for multi-terminal VSC-HVDC transmission lines is that the fault detection and classification can meet the time requirement of a DC circuit breaker (5 ms). The fault location is very accurate and fast enough for online wider system protection and control tasks. This method is designed specifically for MTDC systems, and thus shown to be robust to faults on other lines. In addition, any sections of the post-fault signal can be used, unlike the travelling-wave methods that use only the initial wavefront to locate the fault. Finally, the method is robust to high resistance faults. The algorithm is shown to have high reliability and high accuracy, and with correct selection of parameters, has generality in that it may be applied to any MTDC system.

Commented [SLB16]: Insert value… sees above comment

7 References

[1] R. Irnawan, K. Srivastava, and M. Reza, "Fault detection in HVDC-connected wind farm with full converter generator," *International Journal of Electrical Power & Energy Systems,* vol. 64, pp. 833-838, 2015/01/01/ 2015.

[2] V. Fernão Pires, J. Fialho, and J. Fernando Silva, "HVDC transmission system using multilevel power converters based on dual three-phase two-level inverters," *International Journal of Electrical Power & Energy Systems,* vol. 65, pp. 191-200, 2015/02/01/ 2015.

[3] S. Azizi, M. Sanaye-Pasand, M. Abedini, and A. Hassani, "A Traveling-Wave-Based Methodology for Wide-Area Fault Location in Multiterminal DC Systems," *Power Delivery, IEEE Transactions on,* vol. 29, pp. 2552-2560, 2014.

[4] I. D'Adamo and P. Rosa, "Current state of renewable energies performances in the European Union: A new reference framework," *Energy Conversion and Management,* vol. 121, pp. 84-92, 2016.

[5] D. Van Hertem and M. Ghandhari, "Multi-terminal VSC HVDC for the European supergrid: Obstacles," *Renewable and sustainable energy reviews,* vol. 14, pp. 3156-3163, 2010.

[6] L. Tang, B. Wu, V. Yaramasu, W. Chen, and H. S. Athab, "Novel dc/dc choppers with circuit breaker functionality for HVDC transmission lines," *Electric Power Systems Research,* vol. 116, pp. 106-116, 2014.

[7] E. Rakhshani, D. Remon, and P. Rodriguez, "Effects of PLL and frequency measurements on LFC problem in multi-area HVDC interconnected systems," *International Journal of Electrical Power & Energy Systems,* vol. 81, pp. 140-152, 2016/10/01/ 2016.

[8] N. Flourentzou, V. G. Agelidis, and G. D. Demetriades, "VSC-Based HVDC Power Transmission Systems: An Overview," *Power Electronics, IEEE Transactions on*, vol. 24, pp. 592-602, 2009.

[9] O. G.-B. Dirk Van Hertem, Jun Liang, *HVDC Grids: For Offshore and Supergrid of the Future*. IEEE Press series on power engineering, April 2016.

[10] K. Sano and M. Takasaki, "A surgeless solid-state DC circuit breaker for voltage-source-converter-based HVDC systems," *Industry Applications, IEEE Transactions on,* vol. 50, pp. 2690-2699, 2014.

[11] O. Nanayakkara, A. D. Rajapakse, and R. Wachal, "Traveling-wave-based line fault location in star-connected multiterminal HVDC systems," *Power Delivery, IEEE Transactions on,* vol. 27, pp. 2286-2294, 2012.

[12] S.-p. Gao, X. Chu, Q.-y. Shen, X.-f. Jin, J. Luo, Y.-y. Yun*, et al.*, "A novel whole-line quick-action protection principle for HVDC transmission lines using one-end voltage," *International Journal of Electrical Power & Energy Systems,* vol. 65, pp. 262-270, 2015/02/01/ 2015.

[13] O. M. K. K. Nanayakkara, A. D. Rajapakse, and R. Wachal, "Location of DC Line Faults in Conventional HVDC Systems With Segments of Cables and Overhead Lines Using Terminal Measurements," *Power Delivery, IEEE Transactions on,* vol. 27, pp. 279-288, 2012.

[14] K. De Kerf, K. Srivastava, M. Reza, D. Bekaert, S. Cole, D. Van Hertem*, et al.*, "Wavelet-based protection strategy for DC faults in multi-terminal VSC HVDC systems," *Generation, Transmission & Distribution, IET,* vol. 5, pp. 496-503, 2011.

[15] X. Liu, A. Osman, and O. Malik, "Hybrid traveling wave/boundary protection for monopolar HVDC line," *Power Delivery, IEEE Transactions on,* vol. 24, pp. 569-578, 2009.

[16] Z. Xiao-Dong, T. Neng-Ling, J. S. Thorp, and Y. Guang-Liang, "A transient harmonic current protection scheme for HVDC transmission line," *Power Delivery, IEEE Transactions on,* vol. 27, pp. 2278-2285, 2012.

[17] J. Zheng, M. Wen, Y. Chen, and X. Shao, "A novel differential protection scheme for HVDC transmission lines," *International Journal of Electrical Power & Energy Systems,* vol. 94, pp. 171-178, 1// 2018.

[18] M. Farshad and J. Sadeh, "A Novel Fault-Location Method for HVDC Transmission Lines Based on Similarity Measure of Voltage Signals," *Power Delivery, IEEE Transactions on,* vol. 28, pp. 2483-2490, 2013.

[19] Z.-Y. He, K. Liao, X.-P. Li, S. Lin, J.-W. Yang, and R.-k. Mai, "Natural frequency-based line fault location in HVDC lines," *Power Delivery, IEEE Transactions on,* vol. 29, pp. 851-859, 2014.

[20] S. H. Ashrafi Niaki, H. Kazemi Karegar, and M. Ghalei Monfared, "A novel fault detection method for VSC-HVDC transmission system of offshore wind farm," *International Journal of Electrical Power & Energy Systems,* vol. 73, pp. 475-483, 2015/12/01/ 2015.

[21] Y. Hao, Q. Wang, Y. Li, and W. Song, "An intelligent algorithm for fault location on VSC-HVDC system," *International Journal of Electrical Power & Energy Systems,* vol. 94, pp. 116-123, 2018/01/01/ 2018.

[22] Q. Yang, S. Le Blond, R. Aggarwal, Y. Wang, and J. Li, "New ANN method for multi-terminal HVDC protection relaying," *Electric Power Systems Research,* vol. 148, pp. 192-201, 2017.

[23] W. Leterme, J. Beerten, and D. Van Hertem, "Nonunit Protection of HVDC Grids With Inductive DC Cable Termination," *IEEE Transactions on Power Delivery,* vol. 31, pp. 820-828, 2016.

[24] S. Le Blond, R. Bertho, D. Coury, and J. Vieira, "Design of protection schemes for multi-terminal HVDC systems," *Renewable and Sustainable Energy Reviews,* vol. 56, pp. 965-974, 2016.

[25] S. P. Le Blond, Q. Deng, and M. Burgin, "High frequency protection scheme for multi-terminal HVDC overhead lines," in *Developments in Power System Protection (DPSP 2014), 12th IET International Conference on*, 2014, pp. 1-5.

[26] G. Song, X. Chu, X. Cai, S. Gao, and M. Ran, "A fault-location method for VSC-HVDC transmission lines based on natural frequency of current," *International Journal of Electrical Power & Energy Systems,* vol. 63, pp. 347-352, 2014.

[27] Z. Bo, R. K. Aggarwal, A. Johns, H. Li, and Y. Song, "A new approach to phase selection using fault generated high frequency noise and neural networks," *Power Delivery, IEEE Transactions on,* vol. 12, pp. 106-115, 1997.

[28] Y. Guo, M. Kezunovic, and D. Chen, "Simplified algorithms for removal of the effect of exponentially decaying DC-offset on the Fourier algorithm," *Power Delivery, IEEE Transactions on,* vol. 18, pp. 711-717, 2003.

[29] E. C. Ifeachor and B. W. Jervis, *Digital signal processing: a practical approach*: Pearson Education, 2002.

[30] Q.-H. Wu, Z. Lu, and T. Ji, *Protective relaying of power systems using mathematical morphology*: Springer Science & Business Media, 2009.

[31] ABB, "ABB's Hybrid HVDC Circuit Breaker," *http://new.abb.com/about/events/cigre2014/hvdc-breaker,* 2014.

[32] W. Chen, O. Malik, X. Yin, D. Chen, and Z. Zhang, "Study of wavelet-based ultra high speed directional transmission

line protection," *Power Delivery, IEEE Transactions on*, vol. 18, pp. 1134-1139, 2003.

[33] Q. Yang, S. Le Blond, F. Liang, W. Yuan, M. Zhang, and J. Li, "Design and Application of Superconducting Fault Current Limiter in a Multiterminal HVDC System," *IEEE Transactions on Applied Superconductivity,* vol. 27, pp. 1-5, 2017.

[34] A. Wasserrab and G. Balzer, "The significance of frequency-dependent overhead lines for the calculation of HVDC line short-circuit currents," *Electrical Engineering,* pp. 1-11, 2015.

[35] D. Jovcic and K. Ahmed, *High Voltage Direct Current Transmission: Converters, Systems and DC Grids*: John Wiley & Sons, 2015.